



## High Pressure Synthesis of Cuprate Perovskites

D. A. Vander Griend<sup>†</sup> and K. R. Poeppelmeier

Department of Chemistry, Northwestern University  
2145 Sheridan Road, Evanston, IL 60208-3113<sup>\*</sup>

H. Toganoh, M. Azuma and M. Takano

Institute for Chemical Research, Kyoto University  
Uji, Kyoto-Fu, 311 Japan<sup>‡</sup>

As members of the  $ABO_3$  family of oxides, the  $Ln_4Cu_3MoO_{12}$  family of compounds ( $Ln = La, Pr, Nd, \text{ and } Sm$ ) all crystallize in the rare-earth hexagonal structure at ambient pressure. At 6 GPa and 1200 K they transform to layered perovskite structures which are ~15% more dense than their ambient pressure variants. The high-pressure phases exhibit two-dimensional antiferromagnetic ordering above 200 K, which is indicative of pure copper-oxygen layers. The lanthanum analogue can be doped with up to 25% strontium,  $(La/Sr)_4Cu_3MoO_{12}$ . A large decrease in resistivity is observed with doping but the compound does not become metallic or superconducting.

### 1. INTRODUCTION

The structures of oxides with  $ABO_3$  stoichiometry have long been classified by the ionic radii of the large A- and small B-cations among other parameters.<sup>1,2</sup> Particular structures are found to be more or less appropriate for certain cations. The perovskite structure readily accommodates large A-cations and smaller B-cations since it offers a 12-coordinate site for the former and an octahedral site for the latter. If the cations are closer in size, other structures are more appropriate. Specifically, for smaller A-cation size, structures such as the rare-earth  $YMnO_3$  type, ilmenite, and corundum ( $Al_2O_3$ ) become favored. This analysis generally holds true for spherical ions. The A- and B-cations in  $La_4Cu_3MoO_{12}$  are appropriately sized to facilitate the perovskite structure, but form the rare-earth  $YMnO_3$  type at ambient pressure instead.<sup>3</sup> The coordination of the A- and B-cations is octahedral and trigonal

bipyramidal, respectively. Pressure increases the coordination preferences of the constituent ions and a perovskite structure can be stabilized for  $La_4Cu_3MoO_{12}$  at 6GPa.<sup>4</sup> The phase is layered and metastable at ambient pressure, transforming to the ambient pressure phase above 800 °C in air.

$La_4Cu_3MoO_{12}$  contains pure  $CuO_{4/2}$  layers similar to high temperature superconductors and is isomorphic with  $La_2CuSnO_6$ , the only fully-oxygenated layered cuprate perovskite to form at ambient pressure. The layers of  $Sn^{IV}$  octahedra have been replaced with mixed  $Cu^{II}$  and  $Mo^{VI}$  octahedra while the pure  $Cu^{II}$  layers remain unsubstituted. High-pressure  $La_4Cu_3MoO_{12}$  exhibits antiferromagnetic spin ordering at 280 K which is indicative of 2-dimensional ordering as seen for  $La_2CuSnO_6$ .<sup>4,5</sup> A second ordering event at 25 K which is not seen for  $La_2CuSnO_6$  corresponds to an antiferromagnetic spin ordering event involving the  $Cu^{II}$  in the mixed layers as well. The layered architecture and the

<sup>†</sup> Supported by a National Science Foundation Graduate Fellowship

<sup>\*</sup> Funding provided by the National Science Foundation (Award No. DMR-9120000) through the Science and Technology Center for Superconductivity at Northwestern University.

<sup>‡</sup>Funding provided by Core Research for Evolutional Science and Technology of Japan Science and Technology Corporation and Grant in Aid for Scientific Research of Ministry of education, Science and Culture.

chemical factors that contribute to its formation in copper perovskites can now be studied by aliovalent and rare-earth substitutions on the La<sup>III</sup> site.

## 2. EXPERIMENTAL

Polycrystalline samples of Ln<sub>4</sub>Cu<sub>3</sub>MoO<sub>12</sub> (Ln = La, Pr, Nd, and Sm) were synthesized at ambient pressure by solid state reaction of stoichiometric amounts of lanthanide oxide, CuO, and MoO<sub>3</sub>. Powders were ground, pressed into pellets (2 metric ton·cm<sup>-2</sup>), and fired at 1025°C in air for four days with two intermittent grindings.

High-pressure samples were synthesized from the ambient pressure phases. Powdered samples were packed in a platinum capsule and pressed under 6 GPa of pressure in a cubic anvil press for thirty minutes at 1200 °C. If the reaction was not complete, then a second attempt was made at 8 GPa and 1400 °C. The details of the procedure have been described elsewhere.<sup>6</sup>

High-pressure strontium doped samples, (La/Sr)<sub>4</sub>Cu<sub>3</sub>MoO<sub>12</sub>, were synthesized from stoichiometric amounts of La<sub>4</sub>Cu<sub>3</sub>MoO<sub>12</sub>, SrO<sub>2</sub>, Sr<sub>2</sub>CuO<sub>3</sub>, CuO, and MoO<sub>3</sub> for 2.5% to 100% strontium. Additional KClO<sub>4</sub> (~1%) was added to the encapsulated sample as a solid oxidizer.

Powder X-ray diffraction (PXD) data for the ambient pressure samples to confirm phase formation and purity were collected every 0.05° for 15° < 2θ < 80° on a Rigaku diffractometer. Data for the high pressure samples were collected every 0.02° for 3° < 2θ < 120° on a Rigaku RINT 2000 diffractometer. Refinement was performed using the Rietveld analysis software Rietan.<sup>7</sup>

Magnetic susceptibility measurements were performed on a Quantum Design Corporation MPMS XL SQUID Susceptometer from 5 to 350 or 400 K.

Four point DC resistivity measurements were made using a Quantum Design PPMS with Ag paint contacts on sintered pellets approximately 3mm in diameter and 1mm thick.

## 3. RESULTS

The ambient pressure samples formed single phases isomorphic to the lanthanum analogue. First mentioned in a preliminary communication,<sup>4</sup> their details will be reported elsewhere. High-pressure Ln<sub>4</sub>Cu<sub>3</sub>MoO<sub>12</sub> formed for Ln = La, Nd, Pr, and Sm.

The structures of the last three are equivalent in connectivity but lower in symmetry than the lanthanum analogue.<sup>4</sup> All are layered. Significant structural trends are consistent with the change in A-cation size. As the A-cation layer shrinks, the *a* and *b* parameters decrease while *c* increases giving an overall decrease in unit cell volume. Also, the compression on the B-cation layers increases with the mismatch between the A-cation and B-cation layers and results in increased buckling within the cuprate planes similar to what was observed in the Ln<sub>2</sub>CuSnO<sub>6</sub> (Ln = La, Pr, and Nd) series.<sup>8</sup> Unit cell parameters for Ln<sub>4</sub>Cu<sub>3</sub>MoO<sub>12</sub> (Ln = La,<sup>4</sup> Nd, Pr, and Sm) are given at the top of Table I.

Figure 1 shows the molar susceptibility of Ln<sub>4</sub>Cu<sub>3</sub>MoO<sub>12</sub> for Ln = Pr and, even though Nd<sup>III</sup>, Pr<sup>III</sup>, and Sm<sup>III</sup> are not spin zero cations, all three samples clearly exhibited a 2-dimensional antiferromagnetic ordering of the Cu<sup>II</sup> spins at high temperature that decreases linearly in temperature with A-cation size (figure 2). The decrease is expected since the increase in the buckling angle within the plane perturbs the spin interaction.<sup>8</sup> The low temperature ordering event also decreases in temperature with cation size.

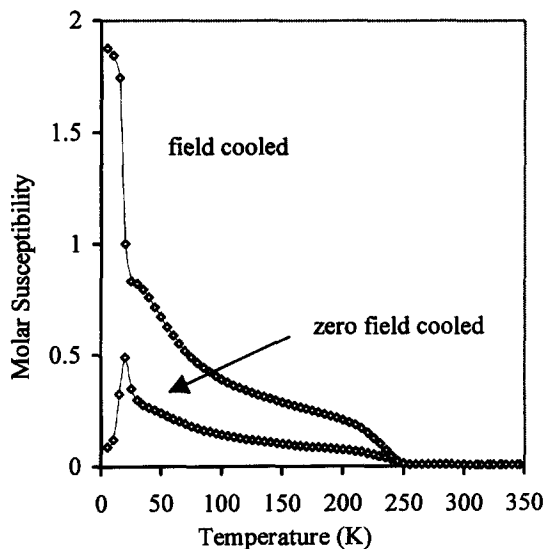


Figure 1. Two transitions at 20 and 250 K can be identified in the temperature dependent molar (per copper) susceptibility for Pr<sub>4</sub>Cu<sub>3</sub>MoO<sub>12</sub>.

Table I

Space group and unit cell parameters for perovskite oxides synthesized under high pressure

Compound	S G	a (Å)	b (Å)	c (Å)	$\alpha$ (°)	$\beta$ (°)	$\gamma$ (°)	Vol (Å <sup>3</sup> )
La <sub>4</sub> Cu <sub>3</sub> MoO <sub>12</sub>	P2 <sub>1</sub> /m	8.233(1)	7.779(1)	7.854(1)	90	92.16(1)	90	502.6
Pr <sub>4</sub> Cu <sub>3</sub> MoO <sub>12</sub>	P-1	8.182(1)	7.653(1)	7.871(1)	90.20(1)	93.60(1)	90.69(1)	491.8
Nd <sub>4</sub> Cu <sub>3</sub> MoO <sub>12</sub>	P-1	8.149(1)	7.611(1)	7.865(1)	90.41(1)	94.12(1)	90.94(1)	486.4
Sm <sub>4</sub> Cu <sub>3</sub> MoO <sub>12</sub>	P-1	8.124(1)	7.590(1)	7.916(1)	90.45(1)	94.81(1)	90.98(1)	486.3
La <sub>3.9</sub> Sr <sub>0.1</sub> Cu <sub>3</sub> MoO <sub>12</sub>	P-1	8.243(1)	7.796(1)	7.854(1)	90.10(1)	91.91(1)	90.78(1)	504.6
La <sub>3.8</sub> Sr <sub>0.2</sub> Cu <sub>3</sub> MoO <sub>12</sub>	P-1	8.162(1)	7.803(1)	7.846(1)	90.02(1)	91.20(1)	90.48(1)	499.5
La <sub>3.6</sub> Sr <sub>0.4</sub> Cu <sub>3</sub> MoO <sub>12</sub>	P-1	8.199(1)	7.794(1)	7.842(1)	90.03(1)	91.29(1)	90.51(1)	500.9
La <sub>3.2</sub> Sr <sub>0.8</sub> Cu <sub>3</sub> MoO <sub>12</sub>	Fm-3m	7.905(1)	7.905(1)	7.905(1)	~90	~90	~90	494
La <sub>3.0</sub> Sr <sub>1.0</sub> Cu <sub>3</sub> MoO <sub>12</sub>	Fm-3m	7.902(1)	7.902(1)	7.902(1)	90	90	90	493.4

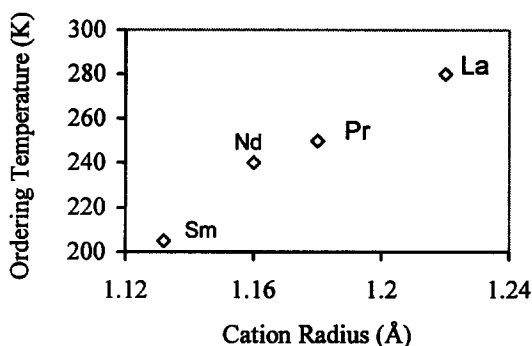


Figure 2. The magnetic ordering temperatures for Ln<sub>4</sub>Cu<sub>3</sub>MoO<sub>12</sub> decrease with Ln<sup>III</sup> size as the Cu-O-Cu bond angle increases (more buckling of planes).

Strontium can be substituted for lanthanum up to 25% in (La/Sr)<sub>4</sub>Cu<sub>3</sub>MoO<sub>12</sub> with concurrent oxidation. Past this point the samples are multiphase. The behavior upon doping is similar to (La/Sr)<sub>2</sub>CuSnO<sub>6</sub>, but considerably more aliovalent substitution occurs. The structure changes drastically from a layered monoclinic perovskite for 0% doping to an isotropic cubic perovskite for 25% doping. The presence of the (1,1,1) peak in the PXD data of this last member suggests that some of the cations are still ordered. One possibility is that the spherical cations, Mo<sup>VI</sup> and Cu<sup>III</sup>, order on every other site as Mn<sup>IV</sup> in La<sub>2</sub>CuMnO<sub>6</sub>.<sup>9</sup> The unit cell parameters converge with increasing doping level, and the volume remains constant for low doping levels before decreasing at higher doping levels.

This is not unexpected since, while Sr<sup>II</sup> is considerably larger than La<sup>III</sup>, hole doping removes an electron from an antibonding orbital localized on the copper. If the Hubbard band splitting of the d<sub>x<sup>2</sup>-y<sup>2</sup></sub> orbital is large enough, then the hole presumably will occur in the d<sub>z<sup>2</sup></sub> orbital.<sup>10</sup> The PXD pattern of the 20% doped material very closely resembles that of the 25% doped one, and both refine well in the cubic space group Fm-3m. The structure of the final member is no longer layered, but more closely resembles a random or rock-salt distribution. The similarity between the last two members of the series suggests that the disappearance of the CuO<sub>4/2</sub> plane owing to the strontium substitution is complete. Structural details are given at the bottom of Table I.

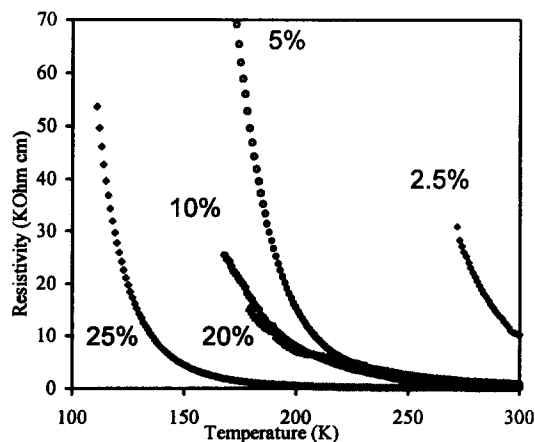


Figure 3. Resistivity as a function of temperature for different doping levels of (La/Sr)<sub>4</sub>Cu<sub>3</sub>MoO<sub>12</sub>.

The resistivity and magnetism of the doped samples are represented in Figures 3 and 4, respectively. Notice that while the samples become increasingly conductive with increase of Sr, they do not become metallic or superconducting. Also, the positive susceptibility, quantified by the high temperature antiferromagnetic ordering is pushed back considerably but approaches a limit as a function of doping. Indeed, the magnetic properties of the more heavily doped samples, like the structures, are comparable. The temperature of the low-temperature ordering event decreases initially with Sr doping and then disappears entirely for all larger doping fractions. This is further evidence that Sr substitution erases the anisotropy of the structure.

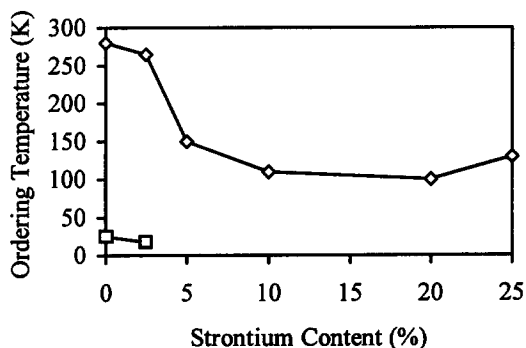


Figure 4. The strength of the magnetic interactions in  $(\text{La}/\text{Sr})_4\text{Cu}_3\text{MoO}_{12}$  decrease as Sr is introduced.

#### 4. CONCLUSIONS

General principles based on size and charge work well to correlate structure with components and allow for a high level of confidence in predicting solid state structures when the ions are spherical. In contrast, high temperature superconductors and other useful oxides that necessarily possess Jahn-Teller cations such as  $\text{Cu}^{\text{II}}$  can not be designed conveniently along these principles. The phases reported here represent a structural crossover within the standard  $\text{ABO}_3$  structures based on spherical ion models. While pressure can be used to stabilize denser structures, it is clear that  $\text{Cu}^{\text{II}}$  destabilizes fully-oxygenated perovskites. The size and the shape of the cation compete to facilitate different structures.  $\text{Cu}^{\text{II}}$  is small enough to form perovskite, but the shape of

the cation is better accommodated by the trigonal bipyramidal sites in the  $\text{YMnO}_3$  structure. As long as three quarters of the B-cations are copper, the  $\text{YMnO}_3$  structure is more stable at ambient pressure for rare-earth A-cations.<sup>4</sup> At high pressure, size accommodations prevail over shape but only with rare-earth A-cations not smaller than Sm. Similarly, when half of the B-cations are copper as in  $\text{Ln}_2\text{CuSnO}_6$ , the perovskite structure only forms at ambient pressure for La. The Pr and Nd analogues form as expected under high-pressure conditions. Larger cations better promote the formation of perovskites rich in  $\text{Cu}^{\text{II}}$ .

The  $\text{Sr}^{\text{II}}$  reaction produces either  $\text{Cu}^{\text{III}}$  or an oxygen vacancy. Both facilitate the incorporation of copper into the perovskite structure. The doping of the molybdate creates a complex charge and bond ordering in these  $\text{Cu}^{\text{II}} / \text{Cu}^{\text{III}} / \text{Mo}^{\text{VI}}$  perovskites. Clearly, further studies are required to determine the precise effect of aliovalent substitution on the dimensionality of both the structure and the electromagnetic properties.

#### REFERENCES

1. D.M. Adams, *Inorganic Solids*; John Wiley & Sons: London, 5 (1974) 105.
2. D.M. Giaquinta and H.-C. zur Loye, *Chem Mater.*, 6 (1994) 365.
3. D.A. Vander Griend, S. Boudin, V. Caignaert, K.R. Poeppelmeier, Y. Wang, V.P. Dravid, M. Azuma, M. Takano, Z. Hu and J. Jorgensen, *J. Am. Chem. Soc.*, 121 (1999) 4787.
4. D.A. Vander Griend, S. Boudin, K.R. Poeppelmeier, H. Toganoh, M. Azuma and M. Takano, *J. Am. Chem. Soc.*, 120 (1998) 11518.
5. M.T. Anderson and K.R. Poeppelmeier, *Chem. Mater.*, 3 (1991) 476.
6. M. Azuma, Z. Hiroi, M. Takano, Y. Bando and Y. Takeda, *Nature*, 356 (1992) 775.
7. Y. Endoh, M. Matsuda, K. Yamada, K. Kakuria, Y. Hidaka, G. Shirane and R. Birgeneau, *J. Phys. Rev.*, B40 (1989) 7023.
8. M. Azuma, S. Kaimori and M. Takano, *Chem. Mater.*, 10 (1998) 3124.
9. M.T. Anderson, K.B. Greenwood, G.A. Taylor, K.R. Poeppelmeier, *Prog. Solid St. Chem.*, 22 (1993) 197.
10. P.A. Salvador, K.B. Greenwood, J.R. Mawdsley, K.R. Poeppelmeier and T.O. Mason, *Chem. Mater.*, 11 (1999) 1760.